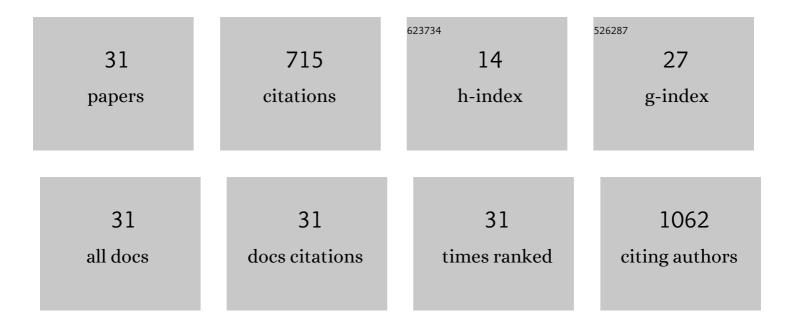
IstvÄjn Kertész

List of Publications by Year in descending order

Source: https://exaly.com/author-pdf/4226291/publications.pdf Version: 2024-02-01



#	Article	IF	CITATIONS
1	A generic gas chromatography method for determination of residual solvents in PET radiopharmaceuticals. Journal of Pharmaceutical and Biomedical Analysis, 2022, 207, 114425.	2.8	4
2	<i>In Vivo</i> Imaging of Ischemia/Reperfusion-mediated Aminopeptidase N Expression in Surgical Rat Model Using ⁶⁸ Ga-NOTA-c(NGR). In Vivo, 2022, 36, 657-666.	1.3	2
3	Preparation, quality control, and biodistribution assessment of [111 In]Inâ€DOTAâ€PR81 in BALB/c mice bearing breast tumors. Journal of Labelled Compounds and Radiopharmaceuticals, 2021, 64, 168-180.	1.0	1
4	In Vivo Molecular Imaging of the Efficacy of Aminopeptidase N (APN/CD13) Receptor Inhibitor Treatment on Experimental Tumors Using 68Ga-NODAGA-c(NGR) Peptide. BioMed Research International, 2021, 2021, 1-11.	1.9	10
5	In vivo preclinical assessment of novel 68Ga-labelled peptides for imaging of tumor associated angiogenesis using positron emission tomography imaging. Applied Radiation and Isotopes, 2021, 174, 109778.	1.5	5
6	Synthesis of 68Ga-Labeled cNGR-Based Glycopeptides and In Vivo Evaluation by PET Imaging. Pharmaceutics, 2021, 13, 2103.	4.5	5
7	Validation and noninvasive kinetic modeling of [¹¹ C]UCB-J PET imaging in mice. Journal of Cerebral Blood Flow and Metabolism, 2020, 40, 1351-1362.	4.3	32
8	In vivo assessment of aminopeptidase N (APN/CD13) specificity of different 68Ga-labelled NGR derivatives using PET/MRI imaging. International Journal of Pharmaceutics, 2020, 589, 119881.	5.2	11
9	<i>In Vivo</i> Imaging of Hypoxia and Neoangiogenesis in Experimental Syngeneic Hepatocellular Carcinoma Tumor Model Using Positron Emission Tomography. BioMed Research International, 2020, 2020, 1-10.	1.9	5
10	Progression of obsessive compulsive disorder-like grooming in Sapap3 knockout mice: A longitudinal [11C]ABP688 PET study. Neuropharmacology, 2020, 177, 108160.	4.1	8
11	In vivo preclinical evaluation of the new 68Ga-labeled beta-cyclodextrin in prostaglandin E2 (PGE2) positive tumor model using positron emission tomography. International Journal of Pharmaceutics, 2020, 576, 118954.	5.2	7
12	Synthesis of ⁶⁸ Ga-Labeled Biopolymer-based Nanoparticle Imaging Agents for Positron-emission Tomography. Anticancer Research, 2019, 39, 2415-2427.	1.1	19
13	Radiochemical synthesis and preclinical evaluation of 68Ga-labeled NODAGA-hydroxypropyl-beta-cyclodextrin (68Ga-NODAGA-HPBCD). European Journal of Pharmaceutical Sciences, 2019, 128, 202-208.	4.0	15
14	Rapid radiosynthesis of two [18 F]″abeled nicotinamide derivatives for malignant melanoma imaging. Applied Radiation and Isotopes, 2018, 132, 142-146.	1.5	0
15	Comparative preclinical evaluation of 68Ga-NODAGA and 68Ga-HBED-CC conjugated procainamide in melanoma imaging. Journal of Pharmaceutical and Biomedical Analysis, 2017, 139, 54-64.	2.8	16
16	<i>In Vivo</i> Imaging of Experimental Melanoma Tumors using the Novel Radiotracer ⁶⁸ Ga-NODAGA-Procainamide (PCA). Journal of Cancer, 2017, 8, 774-785.	2.5	15
17	Multiparametric labeling optimization and synthesis of ⁶⁸ Ga-labeled compounds applying a continuous-flow microfluidic methodology. Journal of Flow Chemistry, 2016, 6, 86-93.	1.9	6
18	The Influence of the Combination of Carboxylate and Phosphinate Pendant Arms in 1,4,7-Triazacyclononane-Based Chelators on Their 68Ga Labelling Properties. Molecules, 2015, 20, 13112-13126.	3.8	15

IstvÃin Kertész

#	Article	IF	CITATIONS
19	In vivo imaging of Aminopeptidase N (CD13) receptors in experimental renal tumors using the novel radiotracer 68Ga-NOTA-c(NGR). European Journal of Pharmaceutical Sciences, 2015, 69, 61-71.	4.0	44
20	2′[18F]-fluoroethylrhodamine B is a promising radiotracer to measure P-glycoprotein function. European Journal of Pharmaceutical Sciences, 2015, 74, 27-35.	4.0	5
21	Efficient synthesis of an (aminooxy) acetylatedâ€somatostatin derivative using (aminooxy)acetic acid as a â€~carbonyl capture' reagent. Journal of Peptide Science, 2011, 17, 39-46.	1.4	32
22	Synthesis and pharmacological characterization of a novel, highly potent, peptidomimetic δ-opioid radioantagonist, [3H]Tyr-Tic-(2S,3R)-β-MePhe-Phe-OH. Neuropeptides, 2008, 42, 57-67.	2.2	5
23	Serial Noninvasive In Vivo Positron Emission Tomographic Tracking of Percutaneously Intramyocardially Injected Autologous Porcine Mesenchymal Stem Cells Modified for Transgene Reporter Gene Expression. Circulation: Cardiovascular Imaging, 2008, 1, 94-103.	2.6	150
24	Novel diastereomeric opioid tetrapeptides exhibit differing pharmacological activity profiles. Brain Research Bulletin, 2007, 74, 119-129.	3.0	11
25	Fluoro-Olefins as Peptidomimetic Inhibitors of Dipeptidyl Peptidases. Journal of Medicinal Chemistry, 2005, 48, 1768-1780.	6.4	136
26	β-Fluorinated proline derivatives: potential transition state inhibitors for proline selective serine dipeptidases. Tetrahedron Letters, 2003, 44, 969-972.	1.4	25
27	Synthesis of (E)- and (Z)-fluoro-olefin analogues of potent dipeptidyl peptidase IV inhibitors. Tetrahedron Letters, 2003, 44, 6231-6234.	1.4	31
28	Binding site of salsolinol: its properties in different regions of the brain and the pituitary gland of the rat. Neurochemistry International, 2003, 42, 19-26.	3.8	42
29	Characterization of N,N(Me)2-Dmt-Tic-OH, a delta selective opioid dipeptide antagonist. NeuroReport, 2000, 11, 2083-2086.	1.2	2
30	Synthesis and binding characteristics of [3H] H-Tyr-TicÏ^[CH2-NH] Cha-Phe-OH, a highly specific and stable δ-opioid antagonist. Peptides, 1999, 20, 1079-1083.	2.4	6
31	Side Chain Methyl Substitution in the δ-Opioid Receptor Antagonist TIPP Has an Important Effect on the Activity Profile. Journal of Medicinal Chemistry, 1998, 41, 5167-5176.	6.4	50